CILAMCE 2017

Florianópolis - Santa Catarina - Brazil

A TOPOLOGICAL DERIVATIVE-BASED METHOD FOR AN INVERSE PROBLEM MODELED BY THE HELMHOLTZ EQUATION

Lucas dos Santos Fernandez

Antonio André Novotny

lucasf@lncc.br

novotny@lncc.br

Laboratório Nacional de Computação Científica LNCC/MCTIC, Coordenação de Matemática Aplicada e Computacional

Avenida Getúlio Vargas 333, 25651-075, Petrópolis, Rio de Janeiro, Brasil

Ravi Prakash

rprakash@udec.cl

Departamento de Matemática, Facultad de Ciencias Físicas y Matemáticas, Universidad de Concepción

Avenida Esteban Iturra s/n, Barrio Universitario, Casilla 160 C, Concepción, Chile

Abstract. *This paper deals with an inverse problem whose forward model is governed by Helmholtz equation. The inverse problem consists in the reconstruction of a set of geometrical subdomains contained in a reference domain from partial measurements of a scalar field of interest. Since the inverse problem, we are dealing with, is written in the form of an ill-posed boundary value problem, the idea is to rewrite it as a topology optimization problem. We are using the concepts of topological derivatives, hence the shape functional measuring the misfit between the known target data and the calculated data is minimized with respect to a set of ball-shaped inclusions. It leads to a non-iterative reconstruction algorithm which is independent of any initial guess. As a result, the reconstruction process becomes very robust with respect to the noisy data. A numerical example is presented in order to demonstrate the effectiveness of the proposed algorithm.*

Keywords: *Inverse problem, Helmholtz equation, Higher-order topological derivatives, Topology optimization, Reconstruction method*

1 INTRODUCTION

In this paper, we study an inverse problem of reconstructing an unknown number ($N^* \in \mathbb{Z}^+$) of isolated geometrical subdomains whitin an open and bounded domain $\Omega \subseteq \mathbb{R}^2$ with smooth boundary $\partial\Omega$. For this purpose, we assume that measurements of a scalar field of interest are taken in a subdomain $\Omega_o \subseteq \Omega$ of domain Ω. We represent each geometrical subdomain by an open connected set $\omega_i^* \subseteq \Omega$ in $\mathbb{R}^2$ such that $\overline{\omega_i^*} \cap \partial\Omega = \emptyset$, $\overline{\omega_i^*} \cap \Omega_o = \emptyset$ and $\overline{\omega_i^*} \cap \overline{\omega_j^*} = \emptyset$ for $i \neq j$ and $i, j \in \{1, \cdots, N^*\}$. If $\omega^* = \cup_{i=1}^{N^*} \omega_i^*$, it is obvious that, for $i = 1, \cdots, N^*$, ω_i^* is an open connected component of ω^* (see Fig. 1(a)).

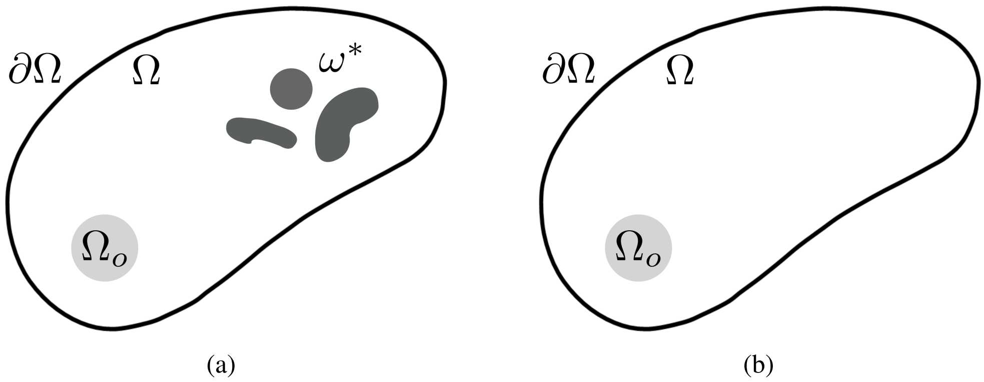

Figure 1: (a) Domain Ω with a set of subdomains ω^* and (b) Domain Ω without subdomains.

To be more precise, for a $k \in \mathbb{R}^+$, we consider the inverse problem consists in finding k_{ω^*} of the form

$$k_{\omega^*} = \begin{cases} 0 & \text{in } \Omega \setminus \omega^*, \\ k & \text{in } \omega^*, \end{cases} \tag{1}$$

which appears in the Helmholtz equation with smooth Robin boundary data on $\partial\Omega$

$$\begin{cases} \Delta z + k_{\omega^*}^2 z &= 0 \quad \text{in } \Omega, \\ \partial_n z + \boldsymbol{i} k z &= g \quad \text{on } \partial\Omega, \end{cases} \tag{2}$$

where $\boldsymbol{i}$ is the imaginary number, i.e., $\boldsymbol{i} = \sqrt{-1}$, n denotes the outward unit normal to the boundary $\partial\Omega$ and z is a scalar field. To solve this problem, we suppose that z is known in Ω_o.

This problem is motivated from the geophysics, Earth science and medical science where scientists try to detect obstructions embedded in a medium by measurements obtained from a wavefield or an electrical field (Carpio & Rapún, 2008, 2012; Feijoo, 2004; Ferreira & Novotny, 2017; Hintermüller *et al.*, 2012). In inverse problems modeled by the Helmholtz equation, for $k, \gamma \in \mathbb{R}^+$, k_{ω^*} has usually the form

$$k_{\omega^*} = \begin{cases} k & \text{in } \Omega \setminus \omega^*, \\ \gamma k & \text{in } \omega^*, \end{cases} \tag{3}$$

and z in Problem (2) represents a wavefield (Carpio & Rapún, 2008, 2012).

The problem (2) with (1) has been selected for its simplicity, e.g., the operator of the governing equation of the problem (2) is independent of k in $\Omega \setminus \omega^*$ and depends on k just in ω^*. This setting makes the treatment of the problem simpler. On the other hand, in contrast to the problem with k_{ω^*} given by (3), the problem with k_{ω^*} given by (1) has no physical meaning. Additionally, the inverse problem (2) does not have a unique solution when we want to determine both, the topology of ω^* and the value of the parameter k. Therefore, in this article, we assume that the value of the parameter k is known and we reconstruct the support of the geometrical subdomain with the help of the measurements of z taken in Ω_o. We proceed by making a guess k_ω of k_{ω^*} as

$$k_\omega = \begin{cases} 0 & \text{in } \Omega \setminus \omega, \\ k & \text{in } \omega, \end{cases} \tag{4}$$

with an open subset $\omega \subseteq \Omega$ such that $\omega \cap \Omega_o = \emptyset$ and $\overline{\omega} \cap \partial\Omega = \emptyset$. Now, we consider u to be the solution of the boundary value problem

$$\begin{cases} \Delta u + k_\omega^2 u &= 0 \quad \text{in } \Omega, \\ \partial_n u + \boldsymbol{i} k u &= g \quad \text{on } \partial\Omega. \end{cases} \tag{5}$$

Since we want our guess k_ω to be close to the unknown k_{ω^*}, it is natural to wish that u approximates z in Ω_o which is known. Keeping this objective in mind, we rewrite our inverse problem in a topology optimization problem observing the well known fact that finding ω^* in (2) for a given $k \in \mathbb{R}^+$ still leads to an ill-posed boundary value problem. Thus, instead to analyse directly (2), we try to solve the topology optimization problem

$$\underset{\omega \subset \Omega}{\text{Minimize}} \;\; \mathcal{J}_\omega\left(u^1, \cdots, u^M\right) = \sum_{m=1}^{M} \int_{\Omega_o} (u^m - z^m)\, \overline{(u^m - z^m)}, \tag{6}$$

which is a weaker formulation of the inverse problem (2). In the minimization problem (6), $M \in \mathbb{Z}^+$ denotes the number of observations, z^m and u^m denotes the known interior data in Ω_o and the solution of the boundary value problem (5), respectively, corresponding to the Robin data g^m, for $m = 1, \cdots, M$. Moreover, $\overline{(u^m - z^m)}$ represents the complex conjugate of $(u^m - z^m)$.

To use the concept of topological derivative, the admissible solution set for the minimization of the problem (6) is considered to be the set of circular subdomains of Ω, i.e., ω appeared in (4) is supposed to be a union of finite number of circular balls. Therefore, the minimizer of (6), denoted by $\omega^\star$ will be only an circular approximation to ω^*. Adopting the method of finding topological derivatives, the shape functional $\mathcal{J}_\omega\left(u^1, \cdots, u^M\right)$ is expanded asymptotically and then truncated up to the desired term to find explicit derivation for topological derivatives of different orders. To develop a non-iterative second order reconstruction algorithm for finding $\omega^\star$, the above mentioned series is trivially minimized with respect to the parameters under consideration. This leads to the highly robustness of the reconstruction process with respect to the noisy data.

The method described above is based on asymptotic expansions which takes into account the concept of topological derivative. This concept was introduced in the fundamental paper by Sokołowski & Żochowski (1999). It has been successfully applied to the treatment of problems such as topology optimization (Amstutz *et al.*, 2012; Lopes *et al.*, 2017), inverse problems (Bonnet, 2009; Canelas *et al.*, 2015; Hintermüller *et al.*, 2012), image processing (Hintermüller & Laurain, 2009), fracture mechanics (Van Goethem & Novotny, 2010; Xavier *et al.*, 2017) and multi-scale constitutive modeling (Amstutz *et al.* 2010). The standard definition of topological derivative leads to first-order iterative methods (Carpio & Rapún, 2008, 2012; Feijoo, 2004) while the simultaneous use of the first and second-order topological derivatives has been allowed to devise a class of second order non-iterative methods (Canelas *et al.*, 2015; Ferreira & Novotny, 2017; Machado *et al.*, 2017). The advantage of methods based on topological derivatives lies in the fact that they are free of any initial guess. Alternatively, in literatures, the level-set methods (Baumeister & Leitão, 2005; Isakov *et al.*, 2011) are available which can be seen as a first-order iterative method. In contrast to the methods based on topological derivatives, their solutions usually depend on the initial guess associated with the level-set initialization. From the characteristics, described earlier in this section, we opted for a method based on the higher-order topological derivatives. In fact, the reconstruction algorithm obtained is non-iterative and independent on the initial guess.

The paper is organized as follows. In Section 2, we recall the notion of topological derivatives and then we introduce some tools related to the theory of topological derivatives needed for the analysis of the inverse problem that we intend to solve. In section 3, the higher-order topological expansion of the shape functional is presented. The non-iterative reconstruction algorithm is devised in Section 4 and a numerical example is presented in Section 5. Finally, in Section 6 the paper ends with some concluding remarks.

2 PRELIMINARIES

In this section, we first recall the concept of topological derivative. Next, we introduce some tools related to the theory of topological derivatives needed for the treatment of the problem of interest.

2.1 Topological derivative concept

The topological derivative measures the sensitivity of a given shape functional with respect to infinitesimal singular domain perturbations such as the insertion of holes, inclusions or cracks. Specifically, an open and bounded domain $\Omega \subset \mathbb{R}^d$, $d \geq 2$, is perturbed by the creation of a small hole $\omega_\varepsilon(\xi)$ of size $\varepsilon > 0$ centred at $\xi \in \Omega$ such that $\overline{\omega_\varepsilon(\xi)} \subset \Omega$. The singularly perturbed domain is denoted by $\Omega_\varepsilon = \Omega \setminus \overline{\omega_\varepsilon(\xi)}$. Then, we assume that a given shape functional $\mathcal{J}(\Omega_\varepsilon)$, associated to the topologically perturbed domain, admits the following topological asymptotic expansion

$$\mathcal{J}(\Omega_\varepsilon) = \mathcal{J}(\Omega) + f(\varepsilon)\, D_T\mathcal{J}(\xi) + o(f(\varepsilon)), \tag{7}$$

where $\mathcal{J}(\Omega)$ is the shape functional associated to the reference (unperturbed) domain Ω. In this expression, the function $\varepsilon \in \mathbb{R}^+ \mapsto f(\varepsilon) \in \mathbb{R}^+$ is smooth and goes to zero with ε. The function $\xi \mapsto D_T(\xi)$ is called the topological derivative of $\mathcal{J}$ at ξ.

Similarly, the second order topological derivative of the shape functional $\mathcal{J}$ at ξ can be obtained by expanding the remainder term $o(f(\varepsilon))$ in Eq. (7). More precisely, we will get the topological asymptotic expansion

$$\mathcal{J}(\Omega_\varepsilon) = \mathcal{J}(\Omega) + f(\varepsilon)\, D_T\mathcal{J}(\xi) + f_2(\varepsilon)\, D_T^2\mathcal{J}(\xi) + o(f_2(\varepsilon)), \tag{8}$$

where the function $\varepsilon \in \mathbb{R}^+ \mapsto f_2(\varepsilon) \in \mathbb{R}^+$ is smooth and it behaves analogously to the function $f(\varepsilon)$ with respect to ε. The function $\xi \mapsto D_T^2(\xi)$ is called the second-order topological derivative of $\mathcal{J}$ at ξ. Furthermore, one can define higher-order topological derivatives by arguing analogically. For a more detailed presentation on the concepts of topological derivatives, we refer the readers to the book by Novotny & Sokołowski (2013), where the authors provide a range of examples in the context of topology optimization.

2.2 Topology optimization setting

Now, taking into account that we are interested in solving the minimization problem given by (6) by using topological derivatives, we draw our attention on two facts very well known in the literatures of topology optimization. First one is that we have to get the asymptotic expansion of $\mathcal{J}_\omega\left(u^1, \cdots, u^M\right)$ up to a predecided order with respect to the parameters depend upon a set of small inclusions (holes or cracks, depending on the problem). Second fact is that the topological derivatives obtained from this expansion has nothing to do with the initial guess of the unknown topology ω^*. Keeping these two facts in mind, we choose $\omega = \emptyset$ as our initial guess and then perturb it by introducing $N \in \mathbb{Z}^+$ number of small circular disjoint inclusions $B_{\varepsilon_i}(x_i)$ with center at $x_i \in \Omega$ and radius ε_i for $i = 1, \cdots, N$ such that $\overline{B_{\varepsilon_i}(x_i)} \cap \overline{B_{\varepsilon_j}(x_j)} = \emptyset$ for each $i \neq j$ and $i, j \in \{1, \cdots, N\}$. If we denote $B_\varepsilon(\xi) = \cup_{i=1}^N B_{\varepsilon_i}(x_i)$ with $\xi = (x_1, \cdots, x_N)$ and $\varepsilon = (\varepsilon_1, \cdots, \varepsilon_N)$, we ask for $\overline{B_\varepsilon} \cap \partial\Omega = \emptyset$ and $\overline{B_\varepsilon} \cap \Omega_o = \emptyset$. For $m = 1, \cdots, M$, suppose u_0^m be the solution of the boundary value problem in an unperturbed domain (see Fig. (1(b)))

$$\left\{\begin{array}{rcll} \Delta u_0^m &=& 0 & \text{in } \Omega, \\ \partial_n u_0^m + \boldsymbol{i} k u_0^m &=& g^m & \text{on } \partial\Omega \end{array}\right. \tag{9}$$

with the corresponding misfit shape functional

$$\mathcal{J}_0\left(u_0^1, \cdots, u_0^M\right) = \sum_{m=1}^{M} \int_{\Omega_o} (u_0^m - z^m)\, \overline{(u_0^m - z^m)}. \tag{10}$$

According to the nature of assumptions on k_{ω^*}, the k_ε for the small circular inclusions will have the form

$$k_\varepsilon = \left\{\begin{array}{ll} 0 & \text{in } \Omega \setminus B_\varepsilon(\xi), \\ k & \text{in } B_\varepsilon(\xi). \end{array}\right. \tag{11}$$

With this k_ε, for $m = 1, \cdots, M$, let u_ε^m be the solution of the perturbed boundary value problem

$$\left\{\begin{array}{rcll} \Delta u_\varepsilon^m + k_\varepsilon^2 u_\varepsilon^m &=& 0 & \text{in } \Omega, \\ \partial_n u_\varepsilon^m + \boldsymbol{i} k u_\varepsilon^m &=& g^m & \text{on } \partial\Omega, \end{array}\right. \tag{12}$$

with the corresponding misfit shape functional

$$\mathcal{J}_\varepsilon\left(u_\varepsilon^1, \cdots, u_\varepsilon^M\right) = \sum_{m=1}^{M} \int_{\Omega_o} (u_\varepsilon^m - z^m)\,\overline{(u_\varepsilon^m - z^m)}. \tag{13}$$

By definition, in the current setting, the topological derivatives measure the sensitivity of the misfit between the known data and the calculated data into the perturbed domain in terms of the size ε and location ξ of the perturbations in the form of a set of small inclusions $B_\varepsilon(\xi)$. In addition, we highlight that any information related to the scalar functions u_0^m, u_ε^m and z^m are known just in the subdomain $\Omega_o \subseteq \Omega$. Using this concept of topological derivatives, in this article, our idea is to obtain the number, size and location of the inclusion which is the best circular approximation to the unknown geometrical subdomain ω^*.

According to Section 2.1, since we have defined the misfit shape functional in the perturbed domain (13) and its unperturbed counter-part (10), a next natural step is to evaluate the difference between these functionals in order to obtain an asymptotic expansion as given in Eq. (8), for example. However, the asymptotic development of the shape functional $\mathcal{J}_\varepsilon\left(u_\varepsilon^1, \cdots, u_\varepsilon^M\right)$ is performed in Section 3.2.

3 TOPOLOGICAL ASYMPTOTIC EXPANSION

Here, we first propose an *ansätz* for the asymptotic expansion of u_ε^m, solution of the problem related to the topologically perturbed domain. Next, with this expansion for u_ε^m, written in terms of u_0^m, solution of the problem related to the unperturbed domain, and other scalar functions, it is possible to proceed with the asymptotic expansion of the shape functional $\mathcal{J}_\varepsilon\left(u_\varepsilon^1, \cdots, u_\varepsilon^M\right)$ from which the reconstruction scheme is devised.

3.1 Asymptotic expansion of the solution

The perturbed shape functional $\mathcal{J}_\varepsilon\left(u_\varepsilon^1, \cdots, u_\varepsilon^M\right)$, given by (13), depends on the small parameter ε through the solution u_ε^m of the problem (12), for $m = 1, \cdots, M$. Therefore, we propose the following *ansätz* for the expansion of u_ε^m with respect to the parameters corresponding to the small circular inclusions as described in Section 2.2

$$u_\varepsilon^m(x) = u_0^m(x) + k^2 \sum_{i=1}^{N} |B_{\varepsilon_i}(x_i)|\, h_i^{\varepsilon,m}(x) + k^4 \sum_{i=1}^{N}\sum_{j=1}^{N} |B_{\varepsilon_i}(x_i)|\,|B_{\varepsilon_j}(x_j)|\, h_{ij}^{\varepsilon,m}(x) + \tilde{u}_\varepsilon^m(x), \tag{14}$$

where $|B_{\varepsilon_i}(x_i)|$ is the Lebesgue measure (volume) of the two-dimensional ball $B_{\varepsilon_i}(x_i)$, namely, $|B_{\varepsilon_i}(x_i)| = \pi\varepsilon_i^2$. In Eq. (14), the three scalar functions $h_i^{\varepsilon,m}(x)$, $h_{ij}^{\varepsilon,m}(x)$ and $\tilde{u}_\varepsilon^m(x)$ are solutions of boundary value problems. In fact, for each $i, j = 1, \cdots, N$ and $m = 1, \cdots, M$, $h_i^{\varepsilon,m}$ is the solution of

$$\left\{\begin{array}{rcll} \Delta h_i^{\varepsilon,m} &=& -\dfrac{u_0^m}{|B_{\varepsilon_i}(x_i)|}\chi_{B_{\varepsilon_i}(x_i)} & \text{in } \Omega, \\ \partial_n h_i^{\varepsilon,m} + \boldsymbol{i}k h_i^{\varepsilon,m} &=& 0 & \text{on } \partial\Omega, \end{array}\right. \tag{15}$$

the function $h_{ij}^{\varepsilon,m}$ satisfies

$$\begin{cases} \Delta h_{ij}^{\varepsilon,m} &= -\dfrac{h_j^{\varepsilon,m}}{|B_{\varepsilon_i}(x_i)|}\chi_{B_{\varepsilon_i}(x_i)} & \text{in } \Omega, \\ \partial_n h_{ij}^{\varepsilon,m} + \boldsymbol{i}k h_{ij}^{\varepsilon,m} &= 0 & \text{on } \partial\Omega, \end{cases} \tag{16}$$

and $\tilde{u}_\varepsilon^m$ is the solution to the following boundary value problem

$$\begin{cases} \Delta \tilde{u}_\varepsilon^m + k_\varepsilon^2 \tilde{u}_\varepsilon^m &= -\Phi_\varepsilon^m & \text{in } \Omega, \\ \partial_n \tilde{u}_\varepsilon^m + \boldsymbol{i}k \tilde{u}_\varepsilon^m &= 0 & \text{on } \partial\Omega, \end{cases} \tag{17}$$

with

$$\Phi_\varepsilon^m = k^6 \sum_{i=1}^N \sum_{j=1}^N \sum_{l=1}^N |B_{\varepsilon_j}(x_j)||B_{\varepsilon_l}(x_l)| h_{jl}^{\varepsilon,m} \chi_{B_{\varepsilon_i}(x_i)}. \tag{18}$$

The behavior of the function $h_i^{\varepsilon,m}$ with respect to the parameter ε can be analyzed more easily in further calculations if we decompose it as a sum of three functions p_i^ε, q_i and $\tilde{h}_i^{\varepsilon,m}$ in the form

$$h_i^{\varepsilon,m} = u_0^m(x_i)(p_i^\varepsilon + q_i) + \tilde{h}_i^{\varepsilon,m}. \tag{19}$$

The function p_i^ε is solution of the Dirichlet problem

$$\begin{cases} \Delta p_i^\varepsilon &= -\dfrac{1}{|B_{\varepsilon_i}(x_i)|}\chi_{B_{\varepsilon_i}(x_i)} & \text{in } B_R(x_i), \\ p_i^\varepsilon &= -\dfrac{1}{2\pi}\ln R & \text{on } \partial B_R(x_i), \end{cases} \tag{20}$$

with $B_{\varepsilon_i}(x_i) \subset \Omega \subset B_R(x_i)$, $x_i \in \Omega$, $\varepsilon \ll R$. By solving problem (20), one can observe that the solution p_i^ε does not depend on ε outside the ball $B_{\varepsilon_i}(x_i)$. Taking into account, we use the notation $p_i(x) := p_i^\varepsilon(x)$, $\forall x \in \Omega \setminus \overline{B_{\varepsilon_i}(x_i)}$. Additionally, q_i is the solution to the homogeneous boundary value problem

$$\begin{cases} \Delta q_i &= 0 & \text{in } \Omega, \\ \partial_n q_i + \boldsymbol{i}k q_i &= -\partial_n p_i - \boldsymbol{i}k p_i & \text{on } \partial\Omega, \end{cases} \tag{21}$$

and $\tilde{h}_i^{\varepsilon,m}$ solves the boundary value problem

$$\begin{cases} \Delta \tilde{h}_i^{\varepsilon,m} &= -\dfrac{u_0^m - u_0^m(x_i)}{|B_{\varepsilon_i}(x_i)|}\chi_{B_{\varepsilon_i}(x_i)} & \text{in } \Omega, \\ \partial_n \tilde{h}_i^{\varepsilon,m} + \boldsymbol{i}k \tilde{h}_i^{\varepsilon,m} &= 0 & \text{on } \partial\Omega. \end{cases} \tag{22}$$

Taking into account that p_i^ε, solution of the problem (20), depends on ε just inside the ball $B_{\varepsilon_i}(x_i)$, we introduce the following notation from the decomposition proposed in (19)

$$h_i^{\varepsilon,m} := \begin{cases} u_0^m(x_i) h_i^\varepsilon + \tilde{h}_i^{\varepsilon,m} & \text{in } B_{\varepsilon_i}(x_i), \\ u_0^m(x_i) h_i + \tilde{h}_i^{\varepsilon,m} & \text{in } \Omega \setminus \overline{B_{\varepsilon_i}(x_i)}, \end{cases} \tag{23}$$

where

$$h_i^\varepsilon := p_i^\varepsilon + q_i \quad \text{and} \quad h_i := p_i + q_i. \tag{24}$$

Moreover, in order to simplify further analysis, we also introduce an adjoint state v^m as the solution of the following auxiliary boundary value problem

$$\left\{ \begin{array}{rcll} \Delta v^m &=& (u_0^m - z^m)\, \chi_{\Omega_o} & \text{in } \Omega, \\ \partial_n v^m - \boldsymbol{i} k v^m &=& 0 & \text{on } \partial\Omega, \end{array} \right. \tag{25}$$

and to simplify the notation we write

$$\alpha = (\alpha_1, \cdots, \alpha_N) \quad \text{with} \quad \alpha_i := |B_{\varepsilon_i}(x_i)| \tag{26}$$

which allows us to rewrite the *ansätz* (14) as

$$u_\varepsilon^m(x) = u_0^m(x) + k^2 \sum_{i=1}^N \alpha_i h_i^{\varepsilon,m}(x) + k^4 \sum_{i=1}^N \sum_{j=1}^N \alpha_i \alpha_j h_{ij}^{\varepsilon,m}(x) + \tilde{u}_\varepsilon^m(x). \tag{27}$$

3.2 Asymptotic expansion of the shape functional

From the *ansätz* for u_ε^m given by (27), we can obtain the asymptotic expansion of the shape functional $\mathcal{J}_\varepsilon\left(u_\varepsilon^1, \cdots, u_\varepsilon^M\right)$ defined through (13) with respect to ε. However, since we have introduced the notation given by (26), the asymptotic development of the shape functional will be written in terms of α. For this purpose, let us start considering the difference between the perturbed shape functional $\mathcal{J}_\varepsilon\left(u_\varepsilon^1, \cdots, u_\varepsilon^M\right)$ and its unperturbed counter-part $\mathcal{J}_0\left(u_0^1, \cdots, u_0^M\right)$ defined in (13) and (10), respectively, which yields to the following simplified expression

$$\mathcal{J}_\varepsilon(u_\varepsilon) - \mathcal{J}_0(u_0) = \sum_{m=1}^M \int_{\Omega_o} [2\Re\{(u_\varepsilon^m - u_0^m)\overline{(u_0^m - z^m)}\} + (u_\varepsilon^m - u_0^m)\overline{(u_\varepsilon^m - u_0^m)}], \tag{28}$$

where $u_\varepsilon = \left(u_\varepsilon^1, \cdots, u_\varepsilon^M\right)$, $u_0 = \left(u_0^1, \cdots, u_0^M\right)$ and $\Re\{\,\cdot\,\}$ denotes the real part of $\{\,\cdot\,\}$.

By using (27) in (28), we get

$$\begin{aligned} \mathcal{J}_\varepsilon(u_\varepsilon) - \mathcal{J}_0(u_0) \;=\;& 2k^2 \sum_{m=1}^M \sum_{i=1}^N \alpha_i \int_{\Omega_o} \Re\{h_i^{\varepsilon,m}\overline{(u_0^m - z^m)}\} \\ &+ 2k^4 \sum_{m=1}^M \sum_{i=1}^N \sum_{j=1}^N \alpha_i\alpha_j \int_{\Omega_o} \Re\{h_{ij}^{\varepsilon,m}\overline{(u_0^m - z^m)}\} \\ &+ k^4 \sum_{m=1}^M \sum_{i=1}^N \sum_{j=1}^N \alpha_i\alpha_j \int_{\Omega_o} h_i^{\varepsilon,m}\overline{h_j^{\varepsilon,m}} + o\left(|\alpha|^2\right). \end{aligned} \tag{29}$$

Now, let us introduce the weak formulation of the adjoint problem (25) to find $v^m \in H^1(\Omega)$ such that

$$\int_\Omega \nabla v^m \cdot \nabla \overline{\eta} - \boldsymbol{i} k \int_{\partial\Omega} v^m \overline{\eta} = -\int_{\Omega_o} (u_0^m - z^m)\, \overline{\eta}, \quad \forall \eta \in H^1(\Omega). \tag{30}$$

The weak formulations of the boundary value problems (15) and (16) are to find $h_i^{\varepsilon,m} \in H^1(\Omega)$ such that

$$\int_\Omega \nabla h_i^{\varepsilon,m} \cdot \nabla \overline{\eta} + \boldsymbol{i}k \int_{\partial\Omega} h_i^{\varepsilon,m} \overline{\eta} = \frac{1}{\alpha_i} \int_{B_{\varepsilon_i}(x_i)} u_0^m \overline{\eta}, \quad \forall \eta \in H^1(\Omega) \tag{31}$$

and $h_{ij}^{\varepsilon,m} \in H^1(\Omega)$ such that

$$\int_\Omega \nabla h_{ij}^{\varepsilon,m} \cdot \nabla \overline{\eta} + \boldsymbol{i}k \int_{\partial\Omega} h_{ij}^{\varepsilon,m} \overline{\eta} = \frac{1}{\alpha_i} \int_{B_{\varepsilon_i}(x_i)} h_j^{\varepsilon,m} \overline{\eta}, \quad \forall \eta \in H^1(\Omega), \tag{32}$$

respectively.

By choosing $\eta = h_i^{\varepsilon,m}$ in (30) and $\eta = v^m$ in (31) as test functions and then considering the real part of the respective resulting equalities, we obtain

$$\int_{\Omega_o} \Re\{h_i^{\varepsilon,m} \overline{(u_0^m - z^m)}\} = -\frac{1}{\alpha_i} \int_{B_{\varepsilon_i}(x_i)} \Re\{u_0^m \overline{v^m}\}. \tag{33}$$

Similarly, if we choose $\eta = h_{ij}^{\varepsilon,m}$ in (30) and $\eta = v^m$ in (32) as test functions and then we consider the real part of the respective resulting equalities, it gives

$$\int_{\Omega_o} \Re\{h_{ij}^{\varepsilon,m} \overline{(u_0^m - z^m)}\} = -\frac{1}{\alpha_i} \int_{B_{\varepsilon_i}(x_i)} \Re\{h_j^{\varepsilon,m} \overline{v^m}\}. \tag{34}$$

By using (33) and (34) in (29), we obtain

$$\begin{aligned} \mathcal{J}_\varepsilon(u_\varepsilon) - \mathcal{J}_0(u_0) \;=\; & -2k^2 \sum_{m=1}^{M} \sum_{i=1}^{N} \int_{B_{\varepsilon_i}(x_i)} \Re\{u_0^m \overline{v^m}\} \\ & -2k^4 \sum_{m=1}^{M} \sum_{i=1}^{N} \sum_{j=1}^{N} \alpha_j \int_{B_{\varepsilon_i}(x_i)} \Re\{h_j^{\varepsilon,m} \overline{v^m}\} \\ & +k^4 \sum_{m=1}^{M} \sum_{i=1}^{N} \sum_{j=1}^{N} \alpha_i \alpha_j \int_{\Omega_o} h_i^{\varepsilon,m} \overline{h_j^{\varepsilon,m}} + o\left(|\alpha|^2\right). \end{aligned} \tag{35}$$

Taking into account the notations introduced in (23), this last equality can be written as

$$\begin{aligned} &\mathcal{J}_\varepsilon(u_\varepsilon) - \mathcal{J}_0(u_0) = -2k^2 \sum_{m=1}^{M} \sum_{i=1}^{N} \int_{B_{\varepsilon_i}(x_i)} \Re\{u_0^m \overline{v^m}\} \\ &-2k^4 \sum_{m=1}^{M} \sum_{i=1}^{N} \sum_{\substack{j=1 \\ j\neq i}}^{N} \alpha_j \int_{B_{\varepsilon_i}(x_i)} \Re\{u_0^m(x_j)\, h_j \overline{v^m}\} - 2k^4 \sum_{m=1}^{M} \sum_{i=1}^{N} \alpha_i \int_{B_{\varepsilon_i}(x_i)} \Re\{u_0^m(x_i)\, h_i^\varepsilon \overline{v^m}\} \\ &+k^4 \sum_{m=1}^{M} \sum_{i=1}^{N} \sum_{j=1}^{N} \alpha_i \alpha_j \int_{\Omega_o} u_0^m(x_i)\, h_i \overline{u_0^m(x_j)\, h_j} + o\left(|\alpha|^2\right). \end{aligned} \tag{36}$$

The result (36) can be simplified further by noting that, in the first and the second terms of (36), we can consider the Taylor's expansions of the functions u_0^m, v^m and h_j around the point x_i, with $\widehat{x}$ being an intermediate point between x and x_i. Let us denote the last nth term of the Taylor's expansion of a function $f(x)$ around x_i by $D^n f(\widehat{x})(x - x_i)^n$, $n \geq 1$, $n \in \mathbb{N}$. In addition, in the third term of (36), we can use the explicit expression for the analytical part p_i^ε of h_i^ε in (24) inside the ball $B_{\varepsilon_i}(x_i)$.

Finally, after taking into account the above mentioned observations along with the decomposition (19) with the fact that u_0^m and v^m are harmonic outside Ω_o, (36) takes the form

$$\begin{aligned}
&\mathcal{J}_\varepsilon(u_\varepsilon) - \mathcal{J}_0(u_0) = \\
&-2k^2 \sum_{m=1}^{M}\sum_{i=1}^{N} \alpha_i \Re\{u_0^m(x_i)\overline{v^m(x_i)}\} + \frac{k^4}{2\pi}\sum_{m=1}^{M}\sum_{i=1}^{N} \alpha_i^2 \log\alpha_i \Re\{u_0^m(x_i)\overline{v^m(x_i)}\} \\
&-\frac{1+\log\pi^2}{4\pi}k^4 \sum_{m=1}^{M}\sum_{i=1}^{N} \alpha_i^2 \Re\{u_0^m(x_i)\overline{v^m(x_i)}\} - 2k^4 \sum_{m=1}^{M}\sum_{i=1}^{N} \alpha_i^2 \Re\{u_0^m(x_i)\overline{v^m(x_i)}q_i(x_i)\} \\
&-\frac{k^2}{2\pi}\sum_{m=1}^{M}\sum_{i=1}^{N} \alpha_i^2 \Re\{\nabla u_0^m(x_i)\cdot\nabla\overline{v^m(x_i)}\} - 2k^4 \sum_{m=1}^{M}\sum_{i=1}^{N}\sum_{\substack{j=1\\ j\neq i}}^{N} \alpha_i\alpha_j \Re\{u_0^m(x_j)h_j(x_i)\overline{v^m(x_i)}\} \\
&+k^4 \sum_{m=1}^{M}\sum_{i=1}^{N}\sum_{j=1}^{N} \alpha_i\alpha_j \int_{\Omega_o} u_0^m(x_i)h_i(x)\overline{u_0^m(x_j)h_j(x)} + o\left(|\alpha|^2\right). \qquad (37)
\end{aligned}$$

The final form of the asymptotic expansion of the shape functional $\mathcal{J}_\varepsilon\left(u_\varepsilon^1, \cdots, u_\varepsilon^M\right)$, given by (37), is used to devise the reconstruction algorithm in the next section. In the current setting, the remainders are all terms of order $o(|\alpha|^2)$. Since these terms are not considered in the mentioned algorithm, they were omitted in this text.

4 RECONSTRUCTION ALGORITHM

The resulting non-iterative reconstruction algorithm based on the expansion (37) is described in this section. The topological asymptotic expansion of the shape functional $\mathcal{J}_\varepsilon(u_\varepsilon)$ given by (37) can be rewritten in the following matrix equation

$$\mathcal{J}(u_\varepsilon) = \mathcal{J}_0(u_0) - \alpha\cdot d(\xi) + G(\xi)\alpha\cdot\mathrm{diag}(\alpha\otimes\log\alpha) + \frac{1}{2}H(\xi)\alpha\cdot\alpha + o(|\alpha|^2), \qquad (38)$$

where the vector $d \in \mathbb{R}^N$ and the matrices $G, H \in \mathbb{R}^{N\times N}$ have the following entries

$$d_i := 2k^2 \sum_{m=1}^{M} \Re\{u_0^m(x_i)\overline{v^m(x_i)}\}, \qquad (39)$$

$$G_{ii} := \frac{k^4}{2\pi}\sum_{m=1}^{M} \Re\{u_0^m(x_i)\overline{v^m(x_i)}\}, \quad G_{ij} = 0, \quad \text{if} \quad i \neq j \qquad (40)$$

and

$$\begin{aligned}
H_{ii} := &-\frac{1+\log\pi^2}{2\pi}k^4 \sum_{m=1}^{M} \Re\{u_0^m(x_i)\overline{v^m(x_i)}\} - 4k^4 \sum_{m=1}^{M} \Re\{u_0^m(x_i)\overline{v^m(x_i)}q_i(x_i)\} \\
&- \frac{k^2}{\pi}\sum_{m=1}^{M} \Re\{\nabla u_0^m(x_i)\cdot\nabla\overline{v^m(x_i)}\} + 2k^4 \sum_{m=1}^{M}\int_{\Omega_o} u_0^m(x_i)h_i\overline{u_0^m(x_i)h_i}, \qquad (41)
\end{aligned}$$

$$H_{ij} := -4k^4 \sum_{m=1}^{M} \Re\{u_0^m(x_j)h_j(x_i)\overline{v^m(x_i)}\} + 2k^4 \sum_{m=1}^{M} \int_{\Omega_o} \Re\{u_0^m(x_i)h_i\overline{u_0^m(x_j)h_j}\}, \quad (42)$$

if $i \neq j$; respectively, for $i, j = 1, \cdots, N$.

Note that the expression on the right-hand side of Eq. (37) depends explicitly on the number N of geometrical subdomains, their positions ξ and sizes α. Thus, let us now introduce the quantity

$$\delta J(\alpha, \xi, N) := -\alpha \cdot d(\xi) + G(\xi)\alpha \cdot \mathrm{diag}(\alpha \otimes \log \alpha) + \frac{1}{2}H(\xi)\alpha \cdot \alpha. \quad (43)$$

After minimizing (43) with respect to α we obtain the following non-linear system

$$(H(\xi) + G(\xi))\,\alpha + 2G(\xi)\mathrm{diag}(\alpha \otimes \log \alpha) = d(\xi) \quad (44)$$

which it is solved by using Newton's method. Observe that, if the quantity α is solution of the mentioned system, then it becomes a function of the locations ξ, that is, $\alpha = \alpha(\xi)$. Now, let us replace the solution $\alpha = \alpha(\xi)$ of Eq. (44) in Eq. (43), to obtain

$$\delta J(\alpha\,(\xi)\,, \xi, N) := -\frac{1}{2}\,(d(\xi) + G(\xi)\alpha(\xi)) \cdot \alpha(\xi). \quad (45)$$

Therefore, the pair of vectors $(\xi^\star, \alpha^\star)$ which minimizes (43) is given by

$$\xi^\star := \underset{\xi \in X}{\mathrm{argmin}} \left\{ -\frac{1}{2}\,(d(\xi) + G(\xi)\alpha(\xi)) \cdot \alpha(\xi) \right\} \quad \text{and} \quad \alpha^\star := \alpha(\xi^\star), \quad (46)$$

where X is the set of admissible locations of the inclusions. Thus, minimizer of (43) is a set of ball-shaped disjoint inclusions denoted by $\omega^\star$ which is completely characterized by the pair $(\xi^\star, \alpha^\star)$. The optimal locations $\xi^\star$ can be trivially obtained from a combinatorial search over all the n-points of the set X and the optimal sizes are given by the second expression in (46). In short, for a given number of inclusions N, our method is able to find in one step their sizes $\alpha^\star$ and their locations $\xi^\star$. For more sophisticated approaches based on meta-heuristic and multi-grid methods, we refer to Machado *et al.* (2017), where the algorithm proposed in this section can be found in pseudo-code format.

5 NUMERICAL RESULT

A numerical example is presented in order to test the reconstruction scheme proposed in the previous section. Given a target domain comprises a set of geometrical subdomains ω^*, our aim is to reconstruct the set ω^* by a set of circular disjoint inclusions from the help of measurements of a known scalar field z^m (related to the target domain), for $m = 1, \cdots, M$, taken in the subdomain $\Omega_o \subseteq \Omega$ where the information is collected. As previously commented, we desire to obtain the location ξ and the size α of each component of the target geometrical subdomain ω^* by assuming that the parameter $k \in \mathbb{R}$ is known.

The geometric domain consists of a unitary disk centered at the origin, namely $\Omega := B_1(0)$, which is discretized using a three-node finite element scheme. After the subdomain Ω_o is constructed, we form a subgrid with a set of feasible nodes X in the remaining domain $\Omega \setminus \Omega_o$ from the original mesh. The combinatorial and exhaustive search is performed in the set X in order to find the optimal size $\alpha^\star$ and location $\xi^\star$ of the inclusions. In addition, since $\alpha^\star = \pi(\varepsilon^\star)^2$, the optimal size of an inclusion can be also represented by its radius $\varepsilon^\star$.

The auxiliary boundary value problems are solved using the original finite element mesh. From these solutions the sensitivities can be numerically evaluated at any point of the mesh. The boundary $\partial\Omega$ is excited by using three functions as Robin data, namely, $g^1 = 1$, $g^2 = x$ and $g^3 = y$.

The proposed reconstruction scheme is also tested in the presence of noisy data. In this case, in order to obtain the noisy synthetic data, the parameter k_{ω^*} is replaced by $k^{\mu}_{\omega^*}(x) = k_{\omega^*}(x) + \mu\tau(x)\|k_{\omega^*}(x)\|_{L^2(\Omega)}$, where $\tau(x)$ is a random variable taking values in the interval $(0,1)$ and μ corresponds to the noise level.

In the figures below, we represented the geometrical subdomain ω^* by black, the subdomain Ω_o where the information is collected by gray and the remaining domain $\Omega \setminus \Omega_o$ by white color.

The example: Reconstruction of a geometrical subdomain consisting of only one circular shape is demonstrated in this example. Additionally, we verify the robustness of the proposed method with respect to the noisy data. Let the subdomain Ω_o be a circular region centred at $(0.3, -0.3)$ with radius $\rho = 0.3$. A circular shape with center located at $x^* = (-0.4, 0.5)$ and with radius $\varepsilon^* = 0.1$ is considered as the target subdomain ω^*. The domain Ω and the subdomains Ω_o and ω^* are illustrated in Fig. 2. The numerical experiments were conducted with $k = 1$. Figure 3 shows us that the target subdomain is reconstructed accurately in the absence of noise from only one observation with the help of Robin data g^1 . Figure 4 illustrates a case where the target domain is corrupted with a noisy synthetic data. For a level of noise $\mu = 50\%$, it is necessary to increase the number of measurements in order to obtain a satisfactory reconstruction of the target subdomain ω^*. In fact, the result illustrated in Fig. 4(b) was obtained when we improve the number of measurements by considering all the Robin data g^1, g^2 and g^3 simultaneously. The quantitative results present in Table 1 confirm that, as the noise level increases, more measurements are needed to ensure an accurate reconstruction of the target subdomain ω^*.

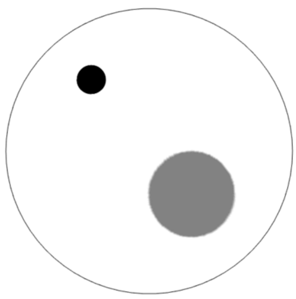

Figure 2: Target domain.

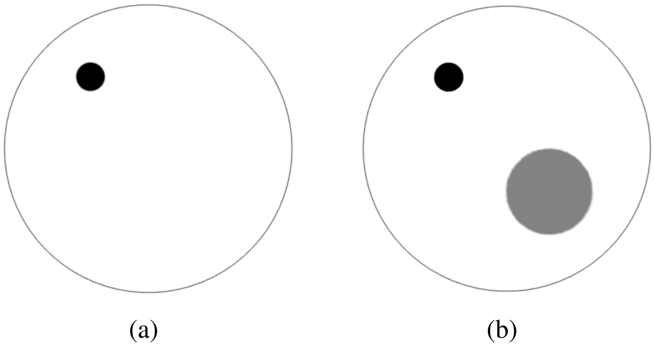

Figure 3: (a) the target domain in the absence of noise $(\mu = 0\%)$ and (b) the obtained reconstruction with $M = 1$.

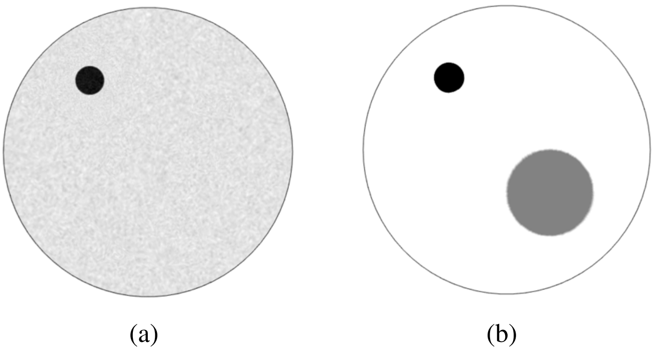

Figure 4: (a) the target corrupted with level noise $\mu = 50\%$ and (b) the obtained reconstruction with $M = 3$.

Table 1: Solutions for different values of μ and M.

		$M = 1$	$M = 2$	$M = 3$
$\mu = 10\%$	$x^\star$	(-0.4,0.5)		
	$\varepsilon^\star$	0.10193		
$\mu = 30\%$	$x^\star$	(-0.32929,0.57071)	(-0.4,0.5)	
	$\varepsilon^\star$	0.10191	0.10377	
$\mu = 50\%$	$x^\star$	(-0.32929,0.57071)	(-0.47071,0.42929)	(-0.4,0.5)
	$\varepsilon^\star$	0.11173	0.098529	0.10446

6 CONCLUSIONS

In this paper a reconstruction method for solving an inverse problem modeled by a Helmholtz equation has been proposed. The reconstruction algorithm is devised from higher-order topological derivatives. In addition, the mentioned algorithm is non-iterative and independent of any initial guess. Hence, the reconstruction process becomes very robust with respect to the noisy data. On the other hand, the approximation of the solution by a finite number of ball-shaped inclusions can be seen as a limitation of our approach. Finally, the ideas from the theory of topological derivatives used here for solving the model problem can be easily extended to more realistic situations, like the one where the problem is given by (2) with parameter k_{ω^*} given by (3).

ACKNOWLEDGEMENTS

This research was partly supported by CNPq (Brazilian Research Council), CAPES (Brazilian Higher Education Staff Training Agency) and FAPERJ (Research Foundation of the State of Rio de Janeiro). These supports are gratefully acknowledged. These research results have also received funding from the EU H2020 Programme and from MCTI/RNP-Brazil under the HPC4E Project, grant agreement n° 689772.

REFERENCES

Amstutz, S., Giusti, S. M., Novotny, A. A., & de Souza Neto, E. A., 2010. Topological derivative for multi-scale linear elasticity models applied to the synthesis of microstructures, *International Journal for Numerical Methods in Engineering*, vol. 84, pp. 733-756.

Amstutz, S., Novotny, A. A., & de Souza Neto, E. A., 2012. Topological derivative-based topology optimization of structures subject to Drucker-Prager stress constraints, *Computer Methods in Applied Mechanics and Engineering*, vol. 233-236, pp. 123-136.

Baumeister, J., & Leitão, A., 2005. *Topics in Inverse Problems*. IMPA Mathematical Publications, Rio de Janeiro.

Bonnet, M., 2009. Higher-order topological sensitivity for 2-D potential problems, *International Journal of Solids and Structures*, vol. 46, n. 11-12, pp. 2275-2292.

Canelas, A., Laurain, A., & Novotny, A. A., 2015. A new reconstruction method for the inverse source problem from partial boundary measurements, *Inverse Problems*, vol. 31, n. 7, pp. 075009.

Carpio, A., & Rapún, M.-L., 2008. Solving inhomogeneous inverse problems by topological derivative methods, *Inverse Problems*, vol. 24, pp. 045014.

Carpio, A., & Rapún, M.-L., 2012. Hybrid topological derivative and gradient-based methods for electrical impedance tomography, *Inverse Problems*, vol. 28, pp. 095010.

Feijoo, G. R., 2004. A new method in inverse scattering based on the topological derivative, *Inverse Problems*, vol. 20, pp. 1819-1840.

Ferreira, A. D., & Novotny, A. A., 2017. A new non-iterative reconstruction method for the electrical impedance tomography problem, *Inverse Problems*, vol. 33, pp. 035005.

Hintermüller, M., & Laurain, A., 2009. Multiphase image segmentation and modulation recovery based on shape and topological sensitivity, *Journal of Mathematical Imaging and Vision*, vol. 35, pp. 1-22.

Hintermüller, M., Laurain, A., & Novotny, A. A., 2012. Second-order topological expansion for electrical impedance tomography, *Advances in Computational Mathematics*, vol. 36, pp. 235-265.

Isakov, V., Leung, S., & Qian, J., 2011. A fast local level set method for inverse gravimetry, *Communications in Computational Physics*, vol. 10, n. 4, pp. 1044-1070.

Lopes, C. G., Santos, R. B., Novotny, A. A., & Sokołowski, J., 2017. Asymptotic analysis of variational inequalities with applications to optimum design in elasticity, *Asymptotic Analysis*, vol. 102, pp. 227-242.

Machado, T. J., Angelo, J. S., & Novotny, A. A., 2017. A new one-shot pointwise source reconstruction method, *Mathematical Methods in the Applied Sciences*, vol. 40, n. 15, pp. 1367-1381.

Novotny, A. A., & Sokołowski, J., 2013. *Topological Derivatives in Shape Optimization*. Interaction of Mechanics and Mathematics. Springer-Verlag, Berlin, Heidelberg.

Sokołowski, J., & Żochowski, A., 1999. On the topological derivative in shape optimization, *SIAM Journal on Control and Optimization*, vol. 37, n. 4, pp. 1251-1272.

Van Goethem, N., & Novotny, A. A., 2010. Crack nucleation sensitivity analysis, *Mathematical Methods in the Applied Sciences*, vol. 33, n. 16, pp. 1978-1994.

Xavier, M., Fancello, E. A., Farias, J. M. C., Van Goethem, N., & Novotny, A. A., 2017. Topological derivative-based fracture modelling in brittle materials: a phenomenological approach, *Engineering Fracture Mechanics*, vol. 179, pp. 13-27.